

Article

Not peer-reviewed version

Finite Black Holes Inside an Eternal Black Hole: Implications for Dark Energy and Dark Matter

[Christopher Laforet](#) *

Posted Date: 9 July 2024

doi: [10.20944/preprints202201.0301.v20](https://doi.org/10.20944/preprints202201.0301.v20)

Keywords: cosmology; black holes; dark energy; Schwarzschild metric



Preprints.org is a free multidiscipline platform providing preprint service that is dedicated to making early versions of research outputs permanently available and citable. Preprints posted at Preprints.org appear in Web of Science, Crossref, Google Scholar, Scilit, Europe PMC.

Copyright: This is an open access article distributed under the Creative Commons Attribution License which permits unrestricted use, distribution, and reproduction in any medium, provided the original work is properly cited.

Disclaimer/Publisher's Note: The statements, opinions, and data contained in all publications are solely those of the individual author(s) and contributor(s) and not of MDPI and/or the editor(s). MDPI and/or the editor(s) disclaim responsibility for any injury to people or property resulting from any ideas, methods, instructions, or products referred to in the content.

Article

Finite Black Holes Inside an Eternal Black Hole: Implications for Dark Energy and Dark Matter

Christopher A. Laforet

Windsor, ON, Canada; claforet@gmail.com

Abstract: The Schwarzschild metric encompasses both exterior and interior regions, with a reversal of signature upon transition from one to the other. Inside the Black Hole, the radial spacelike coordinate transforms into a timelike radius, introducing a time-dependent scale factor on the interior metric's angular term. In this work we consider an infinite, homogeneous distribution of black holes in infinite space. This scenario is a spherically symmetric vacuum and therefore must be described by the Schwarzschild metric. Though the interior metric's is a Kantowski-Sachs type metric, it is shown that the azimuthal scale factor is attributable to Dark Matter effects rather than spatial anisotropy. When considering a Black Hole in the interior metric, we find that as the interior metric's angular basis vector contracts to zero, the inner Black Hole's surface and gravitational field collapse to a point at the singularity. Moreover, we propose a cosmological model wherein the intersection of a Universe and Antiverse spawns FRW Universes, transitioning into Schwarzschild Universes as matter aggregates and spherically symmetric vacua emerge.

Keywords: cosmology; black holes; dark energy; Schwarzschild metric

1. Introduction

The Schwarzschild metric seems to describe two spacetimes separated by an event horizon. The spacetime outside this horizon is well understood and its predictions have been successfully verified over the past century. The spacetime inside the horizon, commonly treated as the spacetime inside a black hole, has been believed to be unobservable to anyone outside of a black hole since light is not able to cross from inside to outside the horizon. As such, it is believed that the predictions associated with this spacetime are untestable.

When moving from the exterior region to the interior, the signature of the metric is reversed such that the timelike coordinate of the external region becomes spacelike in the interior region and likewise for the spacelike coordinate. This means that the radial spacelike coordinate of the exterior region becomes a timelike radius in the interior. This timelike radius has been interpreted as a time-dependant scale factor on the angular term of the metric in the interior.

In this paper, we consider an infinite space with an infinite number of black holes distributed homogeneously throughout space. The vacuum at a location far from any particular black hole will be a spherically symmetric vacuum and therefore must be described by the Schwarzschild metric. It is shown that this vacuum can be modelled as a vacuum with the infinite black holes pushed out to infinity analogous to how we can model the vacuum around a spherically symmetric distribution of matter by concentrating that matter at the center point of the distribution. The result is an infinite vacuum surrounded by an event horizon (formed by the combined horizons of all the surrounding black holes).

We then examine the isotropy of the interior metric and its relationship to Kantowski-Sachs metrics and find that the azimuthal scale factor describes Dark Matter effects rather than a spacelike anisotropy. For the special case of circular motion, the azimuthal scale factor is shown to cause objects with non-zero angular velocity to gain an inertial angular acceleration over time while maintaining its original path through space.

Next, we place a Black Hole inside the interior metric. The vacuum between the Black Hole and outer shell in this case is also a spherically symmetric vacuum and therefore must be described by the Schwarzschild metric. The contraction of the angular term of the interior metric as $r \rightarrow 0$ can be

understood in this case as causing the inner Black Hole, along with its gravitational field, to contract to a point and vanish at $r = 0$. When we put multiple Black Holes homogeneously and isotropically distributed in the interior metric, we can interpret the t coordinate of the interior metric as being the spherically symmetric space between the Black Holes and their gravitational fields.

We present a model of cosmology where the intersection of a Universe/Antiverse pair generates an FRW Universe and Antiverse. This FRW Universe subsequently cools and expands, transitioning into a Schwarzschild Universe as the matter clumps and spherically symmetric vacua emerge between the regions of concentrated matter. This model is compared to cosmological data and it is found that it is capable of accounting for the Dark Energy of the Universe without the need for a cosmological constant.

2. Anisotropy of the Schwarzschild Metric

The Schwarzschild metric has the following form:

$$d\tau^2 = -\left(\frac{u}{r} - 1\right)dt^2 + \frac{1}{\frac{u}{r} - 1}dr^2 - r^2d\Omega^2 \quad (1)$$

The exterior metric, which describes the spacetime around a spherically symmetric mass is given for values of $r > u$ where u is the Schwarzschild radius r_s related to the mass M of the source given by $r_s = 2GM$. This metric treats the mass of the source as being concentrated at point at the center of the spacetime.

So if we have a spherically symmetric distribution of mass in some region, we can model the vacuum outside that region using the exterior Schwarzschild metric with an $r_s = 2GM$ where M is the total mass contained in the region in question. So the vacuum surrounding any finite, static, spherically symmetric volume of mass can be described using the exterior Schwarzschild metric, and the mass is treated as a Black Hole with Schwarzschild radius $2GM$. This metric assumes that there is only a single Black Hole in the spacetime and that the spacetime in which the Black Hole resides is asymptotically Minkowskian.

Now let's consider a different scenario. Suppose we have a spacetime which is infinite in space and has an infinite number of Black Holes homogeneously distributed throughout space. If we take a small, spherical region of empty space somewhere far from any one of the Black Holes, this region will be a spherically symmetric vacuum since all the infinite surrounding Black Holes are distributed homogeneously throughout the surrounding space. This region is therefore a spherically symmetric vacuum which must be described by the Schwarzschild metric. Furthermore, just like we are able to model the vacuum around a spherically symmetric distribution of mass by concentrating that mass at a point in the center of the spacetime, we can likewise model our vacuum surrounded by homogeneously distributed Black Holes as being a vacuum with infinite spatial expanse, surrounded by a continuum of Black Holes infinitely far away. We push the infinite number of Black holes out to spatial infinity and by doing so, their combined event horizons appear as a single event horizon surrounding the vacuum.

This scenario must be described by the Schwarzschild metric because we are describing a spherically symmetric vacuum, and the Schwarzschild metric is the only solution to Einstein's field equation that describes a spherically symmetric vacuum. We know that it cannot be described by the exterior metric because that metric has a Black Hole at its center and is asymptotically Minkowskian (i.e., there are no Black Holes at infinity in the exterior metric). Therefore, this scenario must be described by the interior Schwarzschild metric, which does indeed describe an infinite, spherically symmetric vacuum surrounded by an event horizon.

But given the current understanding of the interior metric, this poses a problem. The interior metric is known as a 'Kantowski-Sachs' spacetime which has different linear and azimuthal scale factors. This is understood to mean that the spacetime is anisotropic. But the hypothetical scenario described above is isotropic since the Black Holes are distributed homogeneously throughout space

and there is no preferred direction when inside the aforementioned vacuum. To reconcile this isotropy problem, we must examine at the Schwarzschild metric in Kruskal-Szekeres coordinates.

The well known Kruskal-Szekeres coordinates, defined in terms of Schwarzschild coordinates are given below. For the exterior metric:

$$\begin{aligned} T &= \sqrt{\left(\frac{r}{r_s} - 1\right)e^{\frac{r}{r_s}}} \sinh\left(\frac{t}{2r_s}\right) \\ X &= \sqrt{\left(\frac{r}{r_s} - 1\right)e^{\frac{r}{r_s}}} \cosh\left(\frac{t}{2r_s}\right) \end{aligned} \quad (2)$$

And for the interior metric:

$$\begin{aligned} T &= \sqrt{\left(1 - \frac{r}{u}\right)e^{\frac{t}{u}}} \cosh\left(\frac{t}{2u}\right) \\ X &= \sqrt{\left(1 - \frac{r}{u}\right)e^{\frac{t}{u}}} \sinh\left(\frac{t}{2u}\right) \end{aligned} \quad (3)$$

We see that we need separate definitions for the exterior and interior metrics, but we can combine these into a single relationship as follows

$$X^2 - T^2 = \left(\frac{r}{u} - 1\right)e^{\frac{r}{u}} \quad (4)$$

Equation 4 is applicable to both the interior and exterior solutions. For the exterior metric, $X^2 - T^2 > 0$ and for the interior solution, $X^2 - T^2 < 0$.

The equation for a 2D hyperboloid surface embedded in three dimensions is given by:

$$\frac{x^2}{a^2} + \frac{y^2}{b^2} - \frac{z^2}{c^2} = \pm 1 \quad (5)$$

For our purposes, we will be considering the special case where $a = b = c$, which gives the one and two sheeted hyperboloids of revolution. Equation 4 appears to be only for one dimension of space, but if we think of X as a radius, then it can describe 3 spherically symmetric dimensions of space.

So comparing to Equation 5, if we set $a^2 = b^2 = c^2 = \left(\frac{r}{u} - 1\right)e^{\frac{r}{u}} \equiv \rho^2$ and $X^2 = R^2 = x^2 + y^2$ where R is a radius of a circle in this example, we obtain an equation that matches the form of Equation 5 where :

$$R^2 - T^2 = \rho^2 \quad (6)$$

Equation 6 describes 2D hyperboloid surfaces for a given r where the interior metric has negative ρ^2 and the exterior metric has positive ρ^2 . Let us now visualize a surface of constant r in both the exterior and interior metrics. For the exterior metric at some $r > r_s$, we get the following hyperboloid of revolution:

On this hyperboloid, the time coordinate t is marked as circles on the sheet and we have one free spatial coordinate ϕ on the surface which is the angle of revolution of the surface. This hyperboloid gives us a clear illustration of anisotropy. Event though we are seeing one dimension of space and one dimension of time on the surface, we can see that moving in one direction along the surface (up and down) is different than moving in the perpendicular direction (around the circumference) because one direction is open and infinite and the other is closed.

This is why it is believed that the interior metric, which has the form of a 'Kntowski-Sachs' spacetime is anisotropic because for the interior metric, the t coordinate is spacelike and if a 2D spacelike foliation of the interior metric were represented by Figure 1, than the t direction of space would be open and infinite, but the perpendicular azimuthal directions would be closed.

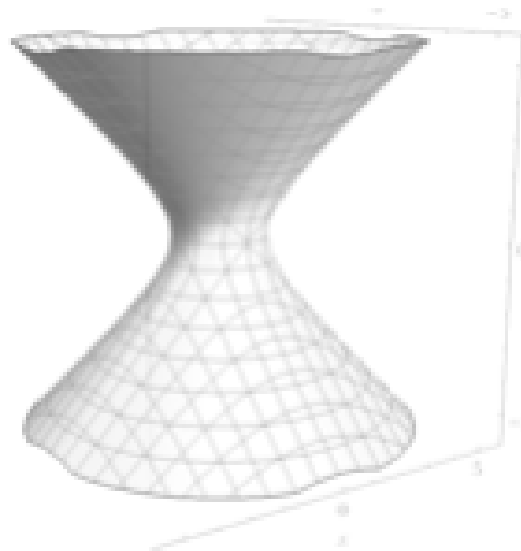


Figure 1. Surface of Constant $r > r_s$ for the Exterior Metric in Kruskal-Szekeres Coordinates

However, we need to recall that for the interior metric, the right side of equation 4 is negative, which gives the following two sheeted hyperboloid surface for some constant $0 < r < u$:

We will discuss the two-sheeted nature of the surface in a later section, but for now let us focus on one of the sheets in terms of spatial isotropy. To help us interpret the surface, it is useful to look at the 2D Kruskal-Szekers coordinate chart:

Let us focus on region II of the chart. Region II is the 1D representation of the upper surface shown in Figure 2. What is important to note in this case is that t is a hyperbolic angle and ∂_t is a Killing vector. This means that we can hyperbolically rotate the spacetime to put any point in region II of the spacetime at $t = 0$ without changing the physics. In other words, any point on a given parabola in region II of Figure 3 can be made the center of the hyperbola by doing a hyperbolic rotation (i.e. there is no intrinsic center for points on the hyperbola, the $t = 0$ point can be any point on the hyperbola). We can say the same with regard to Figure 2. We can move any point on the hyperbola to the 'apex' at $t = 0$ by hyperbolically rotating the surface. So the t coordinate in the metric is akin to a radius for the case where there is no intrinsic spatial center (i.e. one can choose anywhere to be $t = 0$ and then t increases in all directions away from that point).

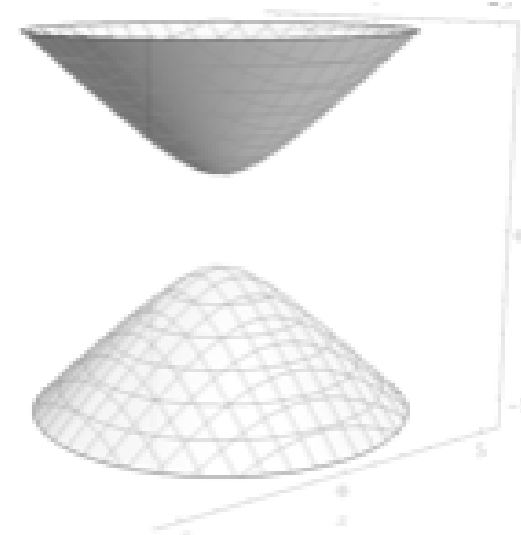


Figure 2. Surface of Constant $0 < r < u$ for the Interior Metric in Kruskal-Szekeres Coordinates

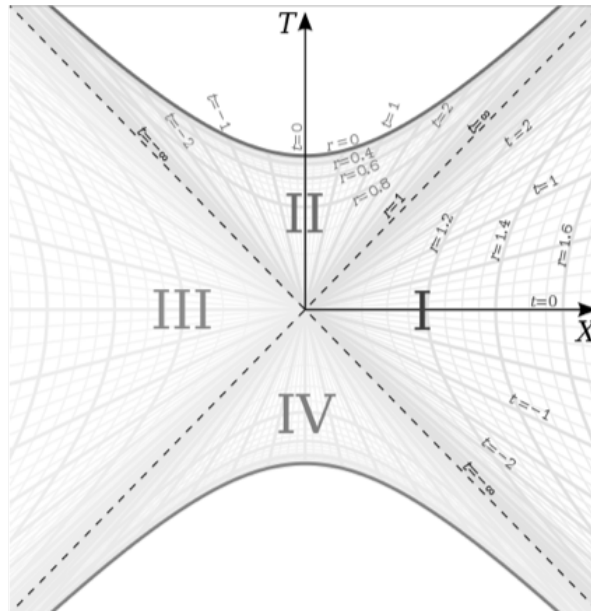


Figure 3. Kruskal-Szekeres Coordinate Chart

So unlike in Figure 1, where the t coordinate is timelike, in Figure 2, representing the interior metric, the t coordinate is spacelike and has no intrinsic center. But the point on the surface at $t = 0$ sees isotropic space since the hyperboloid looks the same in all directions from that point (note that the same is true in 3 dimensions of space, which cannot be represented here. The only difference in 3D is that the circles shown on the surface in Figure 2 are spheres). And since any point can be moved to $t = 0$ arbitrarily, this implies that the vacuum is indeed spatially isotropic, in contrast to the exterior metric.

If the interior metric is spatially isotropic as described above, we must now interpret the azimuthal term of the metric which has a temporal scale factor. As can be seen from the metric in equation 1, as r goes to zero, the ∂_t basis vector becomes infinite while the ∂_ϕ and ∂_θ basis vectors go to zero. We can understand this by imagining two circular paths in the interior vacuum passing through the same point as shown in Figure 4:

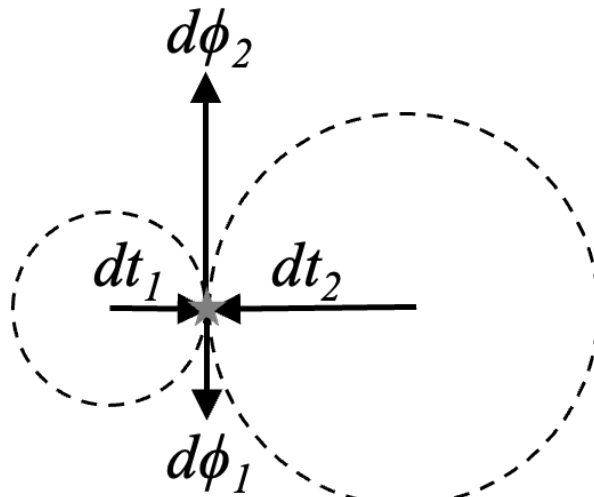


Figure 4. Circular Paths in the Interior Metric

What we see in Figure 4 are two circular paths in the interior metric at some time r centered on two different points but passing through a common point. The $d\phi$ and dt vectors for each path are shown (the particles on each path are travelling counter clockwise). If we were in Minkowski space, the size of these vectors would remain constant over time since the Minkowski metric has no time dependence. But for the interior Schwarzschild metric, the dt vectors would grow and the $d\phi$ vectors would shrink over time as a result of the scale factors in front of those terms in the metric.

The way we can understand this is that if we watch a particle in circular motion in the interior metric, we would see the angular frequency of its motion increase inertially over time while still following the same path without any external forces applied to it. This is because as time passes in the interior metric, r decreases and that causes the ∂_ϕ basis vector to decrease over time such that the circle effectively has a smaller proper circumference over time and therefore it makes a full revolution at a faster rate over time. But the particle does not get closer to the center of the circle over time. Quite the opposite, since the ∂_t basis vector length goes to infinity as r goes to 0, it gets farther from the center point over time while still travelling a shorter path through spaceitme.

This behavior is supported by the geodesic equation for angular motion [1] given below (we will examine the case for planar rotation where $\theta = \frac{\pi}{2}$).

$$\frac{d^2\phi}{d\lambda^2} = -\frac{2}{r} \frac{d\phi}{d\lambda} \frac{dr}{d\lambda} \quad (7)$$

If we choose λ to be r in this analysis and assume an initial circular motion, we can integrate to get the angular velocity $\omega = \frac{d\phi}{dr}$ of the geodesic:

$$\omega = \frac{\omega_0 r_0^2}{r^2} \quad (8)$$

And we see that the angular velocity goes to infinity as r goes to 0. This can be visualized better by looking at the worldline of a circular orbit in the exterior and interior metrics as shown in Figure 5:

On the left side of the figure, we see the circular orbit ($dr = 0$) in the exterior metric with time on the vertical axis and radius on the horizontal axis (a 2D projection of a 3D helix wrapped around the time axis). This a helix with constant radius r . The pitch of the helix is also a constant which means that the angular velocity of the worldline is constant over all time. Since the exterior metric is eternal, this helix can continue as shown for infinite t .

On the right side, we see the same circular orbit ($dt = 0$) in the interior metric. First we note that the signature of the interior metric is flipped relative to the exterior metric and so the vertical time axis is now represented by the r coordinate and the horizontal space axis is represented by the t coordinate. Unlike in the exterior case, the interior metric is finite in time, so the worldline can not go beyond $r = 0$. But we see that the pitch of the helix decreases to 0 as r goes to zero as though the infinite worldline from the exterior metric has been compressed to fit the finite time of the interior metric. A smaller pitch leads to an increasing angular velocity since it implies more rotations per unit time as r goes to zero. Figure 5 therefore shows how the azimuthal scale factor increases the angular velocities of curved geodesics over time without affecting the spatial size of the orbit. This demonstrates how the angular velocity of any size orbit will go to infinity at $r = 0$.

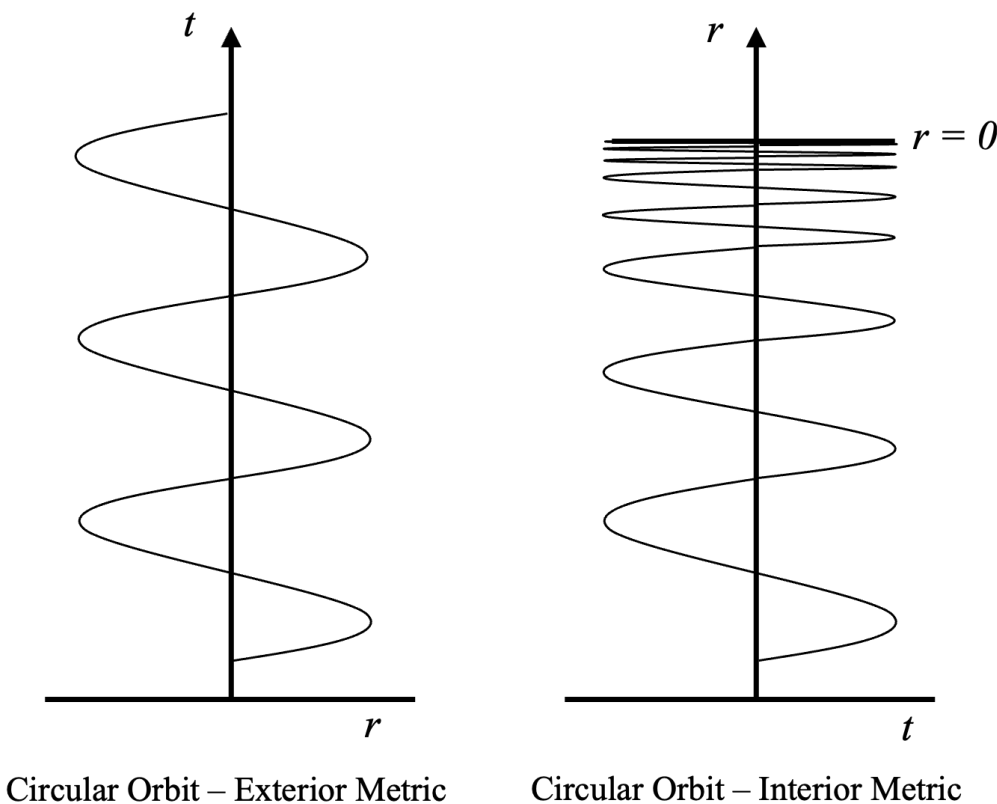


Figure 5. Worldlines of Circular Orbits in the Exterior and Interior Metrics

Therefore, we can interpret the azimuthal scale factor as telling us not that the interior metric is anisotropic, but rather that particles on curved trajectories will experience an angular acceleration over time such that it could take less time to travel on a curved path through space between two points than it would to travel between the same points in a straight line through space.

We will also see in section 4.4 that lensed light experiences the same effect where it causes light bent by massive objects to appear more lensed than the mass of the object alone would imply. Therefore, the Dark Matter effects observed from galaxy rotation curves and excess lensing may be attributable to the fact that the vacuum of the Universe is described by the interior Schwarzschild metric.

We will provide evidence supporting the cosmological interpretation of the interior metric in section 4, but first let us look at what impact the azimuthal scale factor has on the gravitational field of a Black Hole.

3. Finite Black Holes Inside an Infinite Black Hole

It is important to remember that when discussing the interior metric, *t* is the *spacelike coordinate* and *r* is the *timelike coordinate*.

The interior metric describes the interior of a Black Hole. If we place a Black Hole inside the interior metric, the vacuum between the Black Hole and the surface of the shell of the interior metric is also a spherically symmetric vacuum. This can be trivially visualized in Figure 6

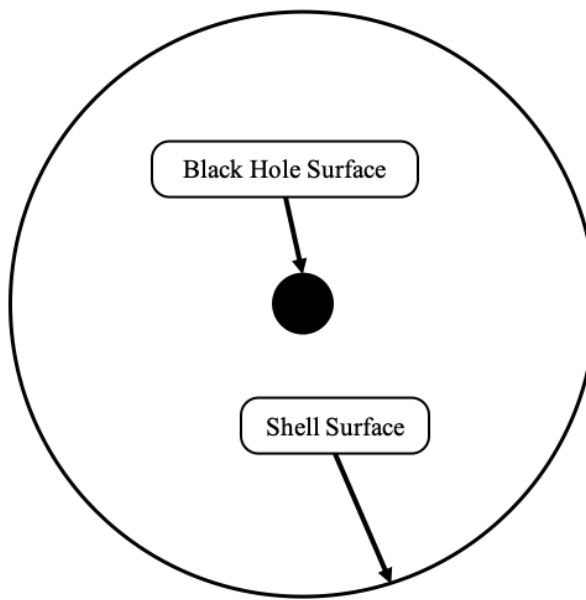


Figure 6. Black Hole inside of a Black Hole

We can see that the vacuum in Figure 6 is spherically symmetric and therefore must also be described by the Schwarzschild metric.

The radial coordinate r of the interior metric is timelike, so as r goes from u to 0, time moves forward. So the Black Hole at the center of Figure 6 is at some $r > 0$ in the interior metric and moves toward $r = 0$ in that metric as time passes. A notable feature of the metric in equation 1 is the angular term $d\Omega$. This term is multiplied by r which goes from u to 0 as time passes. This means that as the Black Hole falls through time in this metric, its surface area will decrease proportionally to r as a consequence of this angular term. At $r = 0$, which is the curvature singularity of the metric, the Black Hole surface area will go to zero, and the Black Hole will no longer exist. It is as though the Black Hole gets squeezed out of existence at the singularity.

If we now imagine that the Black Hole is being orbited by some material, then the contraction of the $d\Omega$ term will also cause those orbits to be squeezed closer to the surface of the Black Hole as time passes. Figure 7 depicts the relative scale of the gravitational field around the Black Hole as it moves through time toward $r = 0$ in the interior metric.

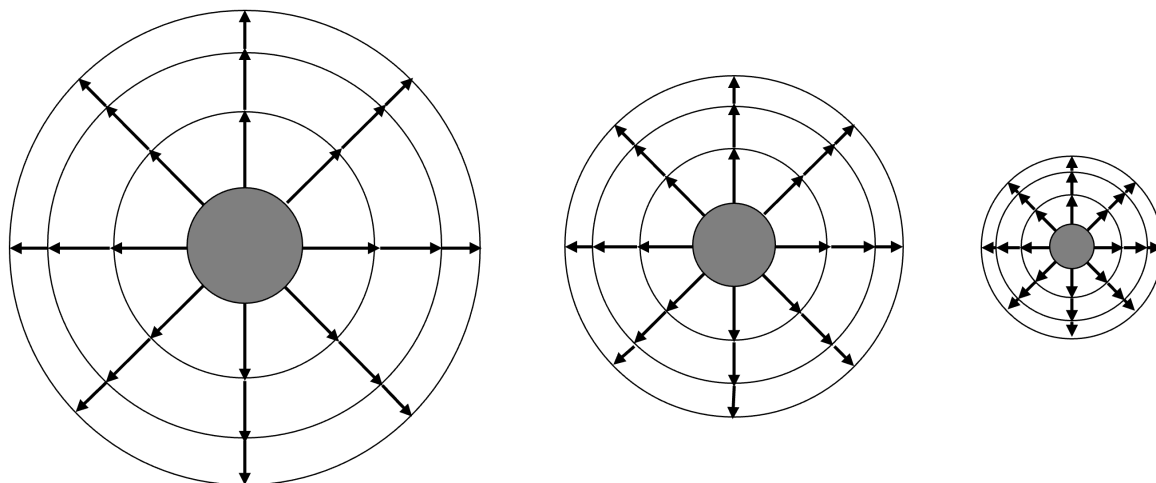


Figure 7. Contraction of a Spherical Gravitational Field and its Orbits in the Interior Metric

According to the interior metric, the dt basis vectors get larger as r decreases, becoming infinite at $r = 0$. Therefore, the proper distance/time between t coordinates increases as the system falls to $r = 0$.

Consider Figure 8 which depicts the curvature of the t coordinates in the exterior metric near the surface of a Black Hole. The t coordinate lines are the curved lines and they come from solving the metric for rest observers ($dr = 0$) and integrating to get the following equation:

$$\tau = t \sqrt{1 - \frac{r_s}{r}} \quad (9)$$

Where each line corresponds to a fixed value of t , with $t = 0$ being the flat line on the r axis. Vertical worldlines on this coordinate chart are the worldlines of observers at rest and their height is the proper time elapsed. We can see that for a given Δt , less proper time passes for rest observers the closer they are to the horizon. The worldlines of observers falling from two different radii are also shown in Figure 8.

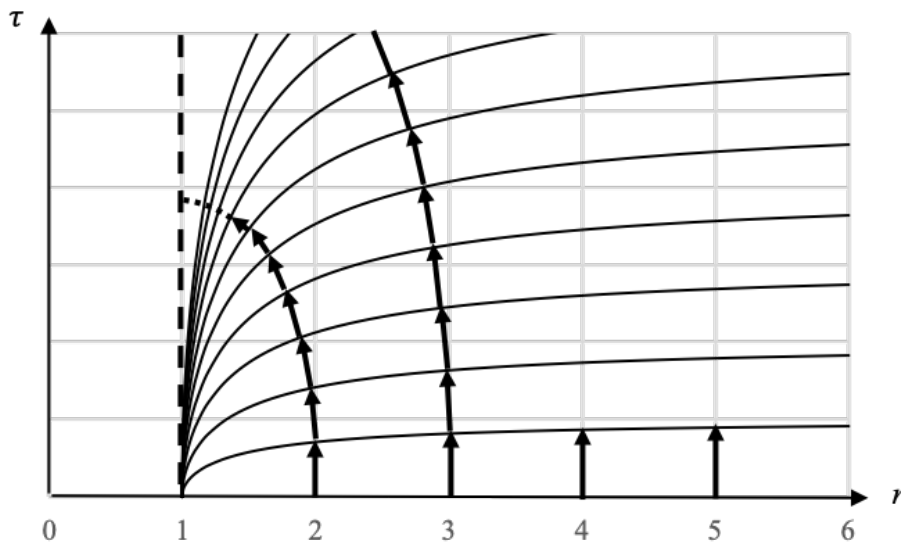


Figure 8. Falling Worldlines on the Modified Schwarzschild Coordinate Chart

We can conceptualize the t coordinate lines as analogous to isocontours on a contour chart, where $t = 0$ represents the highest level and $t = \infty$ represents the lowest level. The trajectory of a falling observer follows the geodesic of shortest distance from the highest level to the lowest level, ensuring their worldline remains perpendicular to the t coordinate lines at every point. Consequently, the worldlines of all falling observers start vertically at $t = 0$, gradually curving to maintain orthogonality to the t coordinate lines at each point, and eventually becoming horizontal at $t = \infty, r = r_s$.

But if the Black Hole is in the interior metric, then the proper time between t coordinate lines will increase as the system falls to $r = 0$ in the interior metric. This has the effect of shifting the gravitational field inward toward the horizon over time as depicted in Figure 9.

The solid t -coordinate lines are the t coordinate lines at some reference time $u > r_0 > 0$ in the interior metric. The dotted lines are the t -coordinate lines at some $r < r_0$ such that those lines are separated by more proper time relative to the solid lines. As shown in Figure 9, this increase in proper distance between coordinate lines shifts the location of a given $\frac{d\tau}{dt}$ closer to the horizon. Since $\frac{d\tau}{dt}$ is related to the acceleration a rest observer feels at a given distance from the horizon, this tells us that the acceleration field is also squeezed toward the horizon as the Black Hole falls toward $r = 0$ in the interior metric.

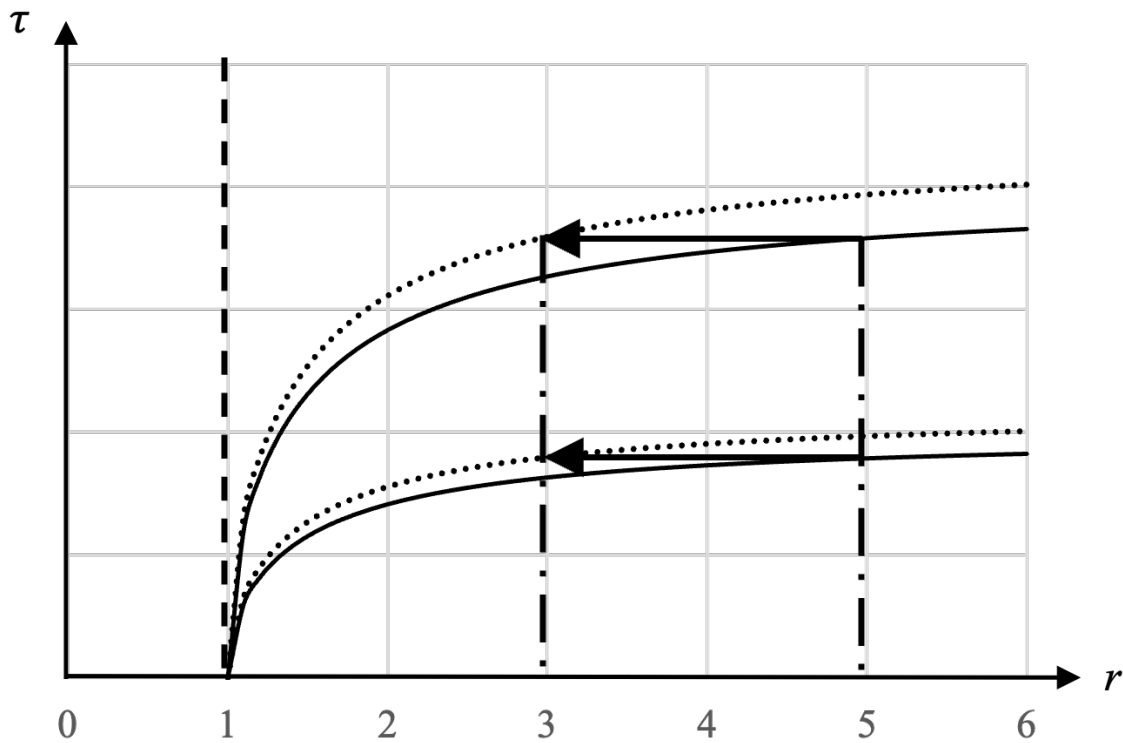


Figure 9. The Shifting of the Gravitational Field from the t Coordinate Expansion

So while the dr and $d\Omega$ terms of the Black Hole system are contracted to a point, the t coordinate far from the Black Hole we placed in the interior metric becomes spacelike and its expansion represents an expansion of space. We can understand this by adding more Black Holes into the shell such that they are distributed homogeneously and isotropically in the infinite space t inside the shell, but separated enough that they do not interact with each other gravitationally. The space between those systems is a vacuum parameterized by the t coordinate of the interior metric.

We will for now focus on region II from Figure 3, where region I captures the external metric and region II captures the interior metric. If we choose some constant value of $r = r_0$ in the interior metric and plot Equation 6 for the interior metric, we get the surfaces shown in the two-sheeted hyperboloid of Figure 2.

Light cones in Figure 2 are oriented vertically and light travels on 45 degree lines. As discussed, we can move any point to the apex of the surface (at $t = 0$) by hyperbolically rotating the spacetime until the point is at the apex. We can do this without changing anything in the spacetime because the hyperbolic rotation is a translation in t , and ∂_t is Killing vector of the manifold. When the point is rotated to the apex, we see then that the light cone is symmetric relative to the surface left and right and into and out of the page. This symmetry means the spacelike foliations of the interior metric's vacuum are isotropic and homogeneous.

This can be extended to three spatial dimensions by allowing R to be the radius of a 3D sphere. In this formulation, we put ourselves at $R = 0$ and the circles on the surfaces in Figure 2 will become spheres that are isotropic and homogeneous in space and inhomogeneous in time, which is consistent with the Cosmological Principle.

So the surface of Figure 2 represents the vacuum of the interior metric with nothing (not even another Black Hole) inside of it. There are no intrinsic spacelike spherical features in this vacuum, and so on its own, it describes a homogeneous space that expands over time (this will be discussed in more detail in section 4). But when we place black holes in this spacetime, they create spacelike spherical regions in the vacuum that contract over time as has been discussed.

We can depict a Black Hole inside the interior metric and better understand the contraction over time with Figure 10.

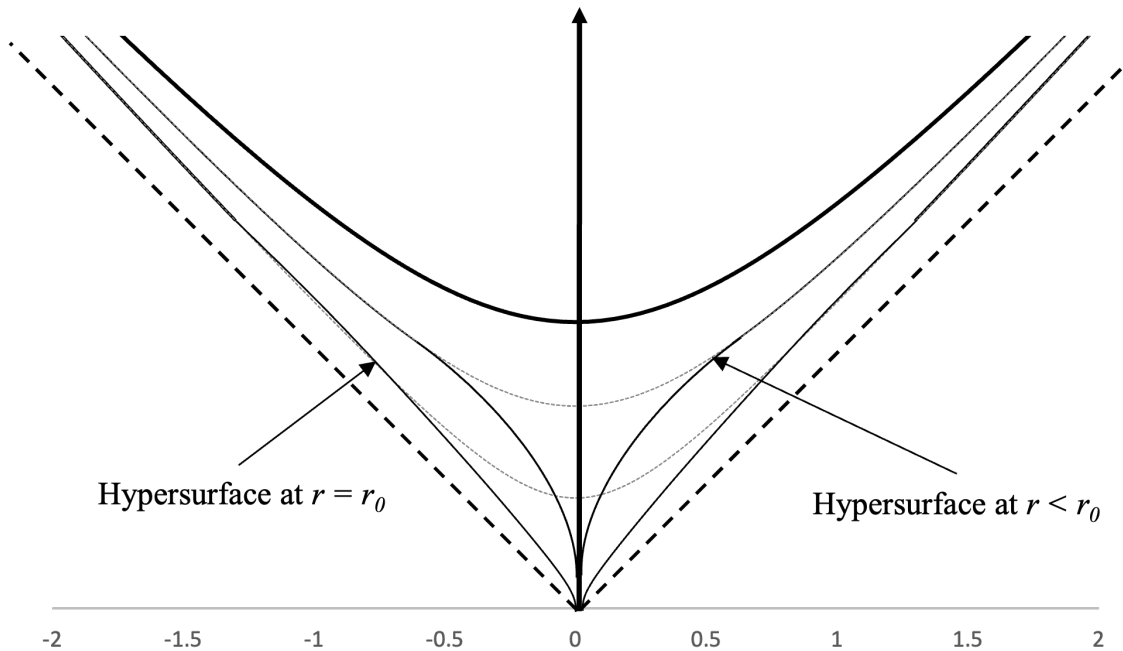


Figure 10. 1-D Visualization of the Distortion of the Interior Vacuum Manifold by a Black Hole

Figure 10 is a modified picture of region II from the Kruskal-Szekeres coordinate chart in Figure 3 with the dark hyperbola representing the singularity at $r = 0$, the 45 degree dashed lines represent the surface of the interior metric, and the hyperbolas between those are the interior vacuum at some $u > r > 0$. We show the Black hole at two different values of r . The undeformed hyperbolas are shown as a dotted line for reference.

So we see from the figure that the gravitational well created by Black Hole can be understood as the spacelike hypersurface $r = r_0$ in the interior spacetime being locally stretched back to the surface of the interior spacetime. Since ∂_t is a Killing vector of the spacetime, we can apply hyperbolic rotations to the hyperbola to make any of the Black Holes homogeneously distributed in the spacetime centered on the diagram. Note that the reason the well stretches back to the $X = T = 0$ point is that at the event horizon, time dilation is infinite. Since the r coordinate is timelike in the interior metric, the r coordinate lines become infinitely dense at the horizon so all the spacelike surfaces of r get pinched to $X = T = 0$ at the Black Hole's event horizon.

The wells stretch out to the surface on the interior region because, as shown in Appendix A, the event horizon of the exterior metric can always be hyperbolically rotated to $X = T = 0$. So it is important to keep in mind that the tips of the wells of the Black Holes at $X = T = 0$ in Figure 10 represent the event horizon of the exterior solution, not the singularity. Furthermore, if we wanted to move from this Black Hole to a different one, we would hyperbolically rotate the space until the other Black Hole was centered at $t = 0$. But that hyperbolic rotation does not move the $X = T = 0$ point, which means that the event horizons of all the infinite Black Holes homogeneously distributed throughout the space are all the same spacetime point $X = T = 0$

Figure 10 shows the vacuum a Black Holes at two times ($u > r_0 > 0$ and a later time $r < r_0$). As the surface moves up toward $r = 0$, the wells narrow and then close at the singularity. This is the contraction of the gravitational field discussed earlier. As the surface moves to $r = 0$, the wells close completely and the spacelike surface becomes completely flat and empty. So the contraction of the dr and $d\Omega$ terms of the internal metric lead to a contraction of the wells and the expansion of the dt term

results in the expansion of the space between the different wells as well as an expansion in the depths of the wells.

A notable point here is that the entire surface, including the wells, represent an interior hypersurface at some r . The meaning of this will be expanded on in section 4, but we should note that as we change the value r of the hypersurface, the relative positions of the wells can change and new wells can be formed at different times (i.e. the hypersurface at some r_0 may have no wells, whereas the same surface at some later time $r < r_0$ can have a well on it if, for instance, a gravitational collapse occurred at some time in between). In fact, we can say that two gravitating systems will combine if they move together more quickly than the t -vacuum between them expands.

Furthermore, we can think of gravitational wells of non-Black Holes, such as a star, as being indents in the hypersurface that do not reach back to the interior surface at a sharp point, those are just smooth, shallower dips in the surface.

It is interesting to think about the interplay of space and time from these gravitational wells. The surface without a Black Hole is perpendicular to the time dimension r in the interior metric. But the gravitational wells stretch that surface in the r direction. Thus, the r direction of the interior region gains spacelike characteristics in the gravitational wells because the spacelike surface gets deformed in the r direction.

We will explore what occurs at the event horizon of the gravitational wells in section 5, but first we will look at this model in the context of the cosmology of the Universe.

4. The Interior Metric as a Model of Cosmology

The interior metric describes a situation where the volume of the space of the vacuum is zero when $r = u$ (because the dt term is zero there), expands over time, and becomes infinite at $r = 0$. This bears a striking resemblance to the Big Bang model of cosmology where the Universe started in an infinitely dense state and subsequently expanded and cooled, condensing into galaxies and gravitational clusters forming a cosmic web surrounding spherically symmetric vacuums of space.

The FRW metric of cosmology describes a perfect fluid with uniform pressure and matter density throughout space which expands over time. This is an adequate description of the Universe in early times when the entire Universe was a hot plasma with uniform density and pressure. But after recombination, The pressure and density of the Universe was no longer uniform. Matter began to clump together into structures creating areas of high and low pressure/density.

We can model cosmology as being described by the FRW metric in the pre-recombination era, but after recombination, the Universe is governed by the Schwarzschild metric. The CMB represents a surface r just inside the shell of the interior Schwarzschild metric, which is a uniform surface that is seen as a surface at the same constant time, regardless of the time r from which it is observed. As will be shown, modelling the Universe in this way will help us resolve the Dark Energy problem without the need for a cosmological constant. This is because the expansion of the t dimension of the interior metric follows a pattern of infinite initial expansion, followed by a period of slowing expansion, followed again by a period of accelerated expansion. This accelerated expansion accounts for the dark energy without the need for a cosmological constant.

If we consider a filament in the cosmic web, which is where most of the matter is but is still mostly vacuum, we can think of the filament as a cylinder that will get stretched along its length and squeezed radially over time. In other words, the cosmic web can be understood as the ongoing 'spaghettification' of the matter in the Universe as it falls toward the singularity at $r = 0$. Furthermore, the contraction of the $d\Omega$ term which puts an inward pressure on the gravitating systems may account for the dark matter observations, but this is left as an area for future research.

It is important to note that this model does not suppose that our Universe exists inside of a Black Hole. Rather, it proposes that the interior metric is the metric of the vacuum of the Universe and there is nothing outside it. Recall that the original assumption when we began discussing the interior metric

was of an infinite Universe with black holes distributed homogeneously. There is no need to assume that the Universe is inside a black hole which is itself part of some external spacetime.

Let us now compare the Schwarzschild cosmological model to cosmological data to show that the model is in very good agreement with experiment.

4.1. The Scale Factor

Expressions for the proper time interval along lines of constant t and Ω and the proper distance interval along hyperbolas of constant r and Ω from Equation 1 are:

$$\frac{ds}{dt} = \pm \sqrt{\frac{u}{r} - 1} = \pm a \quad (10)$$

$$\frac{d\tau}{dr} = \pm \sqrt{\frac{r}{u-r}} = \pm \frac{1}{a} \quad (11)$$

And the coordinate speed of light is given by:

$$\left(\frac{dt}{dr} \right)_{light} = \pm \frac{r}{u-r} = \pm \frac{1}{a^2} \quad (12)$$

Where a is the scale factor (because t is the spatial coordinate and r is the time coordinate and therefore Equation 10 describes how the proper distance between two points separated by coordinate distance dt evolves over time). First we should notice that none of the three equations depend on the t coordinate. This is good because the t coordinate marks the position of other galaxies relative to ours. Since all galaxies are freefalling in time inertially, the particular position of any one galaxy should not matter. The proper temporal velocity, proper distance, and coordinate speed of light only depend on the cosmological time r .

A plot of the scale factor vs. r (with $u = 1$) is given in Figure 11 below:

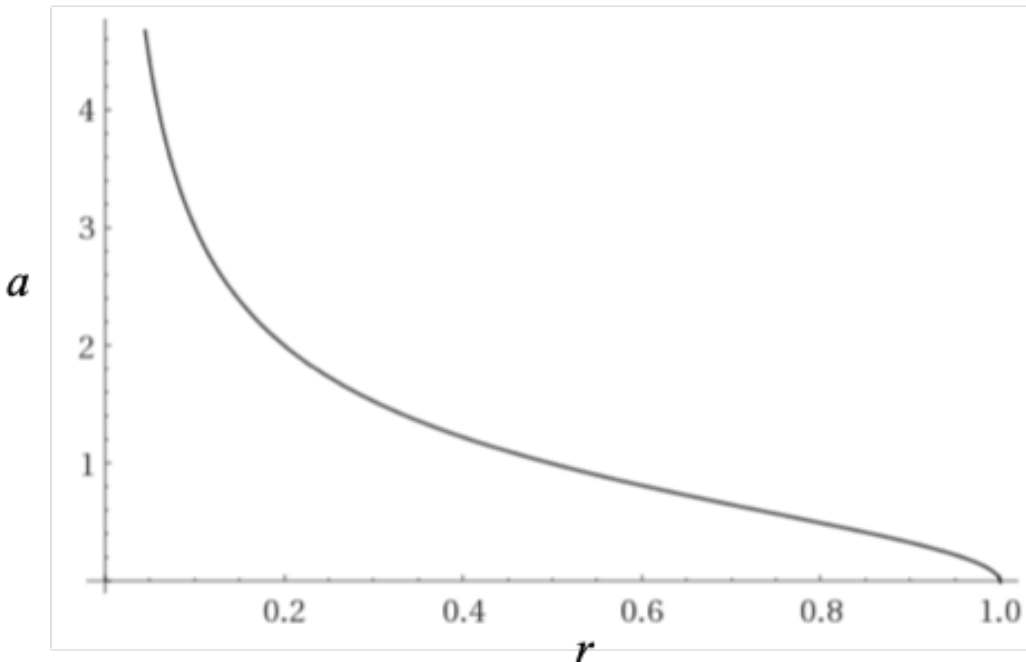


Figure 11. Scale Factor vs. r for $u = 1$

4.2. The Co-Moving Observer

Let us take a co-moving observer somewhere in the Universe we label as $t = 0$ as the origin of an inertial reference frame. We can draw a line through the center of the reference frame that extends infinitely in both directions radially outward. This line will correspond to fixed angular coordinates (Ω). There are infinitely many such lines, but since we have an isotropic, spherically symmetric Universe, we only need to analyze this model along one of these lines, and the result will be the same for any line.

We must determine the paths of co-moving observers ($dt = d\Omega = 0$) in the spacetime. For this we need the geodesic equations for the interior Schwarzschild metric [1] given in Equation 1. In these equations u represents a time constant (in Figure 3, the value of u is 1). The following equations are the geodesic equations of the interior metric for t and r ($0 \leq r \leq u$) for $d\Omega = 0$:

$$\frac{d^2t}{d\tau^2} = \frac{u}{r(u-r)} \frac{dr}{d\tau} \frac{dt}{d\tau} \quad (13)$$

$$\frac{d^2r}{d\tau^2} = \frac{u}{2r^2} \quad (14)$$

Looking at points $0 < r < u$, then by inspection of Equation 13 it is clear that an inertial observer at rest at t will remain at rest at t ($\frac{d^2t}{d\tau^2} = 0$ if $\frac{dt}{d\tau} = 0$).

Let us next demonstrate how the interior metric fits with existing cosmological data and calculate various cosmological parameters using that data.

4.3. Calculation of Cosmological Parameters

In order to compare this model to cosmological data, we must solve for u and find our current position in time (r_0) in the model. Reference [2] gives us transition redshift values ranging from $z_t = 0.337$ to $z_t = 0.89$, depending on the model used. We can use the expression for the scale factor in Equation 10 to get the expression for cosmological redshift from some emitter at r measured by an observer at r_0 [1]:

$$1 + z = \frac{a_0}{a} = \sqrt{\frac{r(u-r_0)}{r_0(u-r)}} \quad (15)$$

Furthermore, the deceleration parameter is given by:

$$q = \frac{\ddot{a}a}{\dot{a}^2} = \frac{4r}{u} - 3 \quad (16)$$

By setting Equation 16 equal to zero, we can solve for $\frac{u}{r}$. With this and equation 10, we can calculate the scale factor at the Universe's transition from decelerating to accelerating expansion a_t :

$$a_t = \sqrt{\frac{4}{3} - 1} = \frac{1}{\sqrt{3}} \quad (17)$$

Using Equations 15, 17, and the transition redshift estimate, we can get an expression for the present scale factor:

$$a_0 = a_t(1 + z_t) = \frac{1 + z_t}{\sqrt{3}} \quad (18)$$

Next, we find expressions for u and our current radius r_0 by noting that light from the CMB has been travelling for roughly 13.8 billion years of coordinate time r . Therefore, we can set $\alpha_{r_0} \equiv u - r_0 = 13.8$ and use Equations 10 and 18 to obtain the following for u and r_0 :

$$r_0 = \frac{u - r_0}{a_0^2} = \frac{\alpha_{r_0}}{a_0^2} = \frac{3\alpha_{r_0}}{(1 + z_t)^2} \quad (19)$$

$$u = r_0 + \alpha_{r_0} = \alpha_{r_0} \left(\frac{3}{(1+z_t)^2} + 1 \right) \quad (20)$$

Next we compute the CMB scale factor (a_{CMB}) and coordinate time (r_{CMB}) in this model where the redshift of the CMB (z_{CMB}) is currently measured to be 1100:

$$a_{CMB} = \frac{a_0}{1+z_{CMB}} \quad (21)$$

$$r_{CMB} = \frac{u}{1+a_{CMB}^2} \quad (22)$$

We can next derive the Hubble parameter equation using the scale factor. The Hubble parameter is given by (in units of $(Gy)^{-1}$):

$$H = \frac{\dot{a}}{a} = \frac{u}{2r(u-r)} \quad (23)$$

Table 1 below gives the values of u , r_0 , H_0 , a_0 , q_0 , a_{CMB} , and q_{CMB} given the upper and lower bounds of z_t from [2] as well as the 0.75 transition redshift value and assuming $\alpha_{r_0} = 13.8$. All times are in Gy and H_0 is in $(km/s)/Mpc$.

Table 1. Limiting Cosmological Parameter Values Based on z_t Measurement and a 13.8 Gy Age of the Universe

z_t	α_{r_0}	u	r_0	H_0	a_0	q_0	a_{CMB}	q_{CMB}
0.337	13.8	37.0	23.2	56.6	0.77	-0.49	0.0007	0.99
0.75	13.8	27.3	13.5	71.6	1.01	-1.02	0.0009	0.99
0.89	13.8	25.4	11.6	77.6	1.09	-1.17	0.0010	0.99

From the results in Table 1, we see that the true transition redshift is likely close to 0.75 given the fact that the current value of the Hubble constant is known to be near 71.6. Thus, more accurate measurements of the transition redshift are needed to increase the confidence of this model, but the 0.75 transition redshift is in fact a prediction of the model and we will see this when it is compared to astronomical data later in this section.

Table 2 has the proper times from $r = u$ to the current time for co-moving observers ($dt = rd\Omega = 0$) by integrating Equation 1. The column τ_{tot} gives the time from $r = u$ to $r = 0$. The expression for τ_{tot} turns out to be quite simple:

$$\tau_{tot} = \frac{\pi}{2}u \quad (24)$$

In Table 2 below, the column τ_{remain} gives the time between $r = r_0$ and $r = 0$.

Table 2. Limiting Proper Times Based on z_t Measurements and an age of 13.8 Gy for the Universe (Time is in Gy)

z_t	α_{r_0}	τ_0	τ_{tot}	τ_{remain}
0.337	13.8	42.2	58.1	15.9
0.75	13.8	35.2	42.9	7.7
0.89	13.8	33.7	39.9	6.2

Note that the proper time τ_0 of the current age of the Universe is actually much larger than the coordinate time $u - r_0$. And even though we are presently only about halfway through the “coordinate life” of the Universe (according to Table 1), the amount of proper time remaining is actually much less than the amount of proper time that has already passed (according to Table 2). This provides a measurable prediction from the model: as telescopes such as the JWST peer farther into the past with greater accuracy, we should expect to find stars, galaxies, and structures that are much older than expected because of the increased amount of proper time available for such things to form in the early

Universe. Hints of this has already been found with the star HD 140283, whose age is estimated to be nearly the age of the Universe itself [3].

Next we would like to use the u and r_0 values found to compare the model to measured supernova and quasar data. First we need to find r as a function of redshift. We can do this by solving for r in Equation 15:

$$r = \frac{u(1+z)^2}{a_0^2 + (1+z)^2} \quad (25)$$

We can derive the expression for t vs. r along a null geodesic where the geodesic ends at the current time r_0 and $t = 0$ by setting $d\tau = rd\Omega = 0$ in Equation 1 and integrating:

$$t = \int_{r_0}^r \frac{r}{u-r} dr = u \ln\left(\frac{u-r_0}{u-r}\right) + r_0 - r \quad (26)$$

Next we substitute Equation 25 into Equation 26 to get coordinate distance in terms of redshift:

$$t = r_0 + u \left[\ln\left(\frac{a_0^2 + (1+z)^2}{1+a_0^2}\right) - \frac{(1+z)^2}{a_0^2 + (1+z)^2} \right] \quad (27)$$

We need to convert the distance from Equation 27 to the distance modulus, μ , which is defined as:

$$\mu = 5 \log_{10}\left(\frac{D_L}{10}\right) \quad (28)$$

Where D_L in Equation 28 is the luminosity distance. Luminosity distance is inversely proportional to brightness B via the relationship:

$$B \propto \frac{1}{D_L^2} \quad (29)$$

The brightness is affected by two things. First, the spatial expansion will effectively increase the distance between two objects at fixed co-moving distance from each other. This will reduce the brightness by a factor of $(1+z)^2$ (because the distance in Equation 29 is squared). But there is also a brightening effect caused by the acceleration in the time dimension. We define $v \equiv \frac{dt}{dr} = \frac{1}{a}$ as the temporal velocity of the inertial observer at some r and the speed of light at that r as $v_c \equiv \frac{dt}{dr} = \frac{1}{a^2}$. The ratio of these velocities gives us:

$$\frac{v_c}{v} = \frac{dt}{dr} \frac{dr}{d\tau} = \frac{dt}{d\tau} = \frac{a}{a^2} = \frac{1}{a} \quad (30)$$

Equation 30 tells us how far a photon travels over a given period of time measured by the inertial observer's clock. So we see that as light travels from the emitter to the receiver, this speed decreases. This decrease in the speed from emitter to receiver will result in an increased photon density at the receiver relative to the emitter, increasing the brightness. Therefore, this effect will increase the brightness by a factor of:

$$\frac{a_0}{a} = 1+z \quad (31)$$

This effect is not accounted for in the current relativistic cosmological models and therefore gives a second prediction that light from the distant Universe should appear brighter than expected.

Taking these brightness effects into account, the total brightness will be reduced by an overall factor of $1+z$ relative to the case of an emitter and receiver at rest relative to each other in flat spacetime. Equation 29 in terms of co-moving distance t and redshift z becomes:

$$B \propto \frac{1+z}{(t(1+z))^2} \rightarrow B \propto \frac{1}{t^2(1+z)} \quad (32)$$

Giving the luminosity distance as a function of co-moving distance t and redshift z :

$$D_L = t\sqrt{1+z} \quad (33)$$

Which gives us the final expression for the distance modulus as a function of co-moving distance and redshift:

$$\mu = 5 \log_{10} \left(\frac{t\sqrt{1+z}}{10} \right) \quad (34)$$

A plot of distance modulus vs. redshift is shown in Figure 12 below plotted over data obtained from the Supernova Cosmology Project [4]. A Curve calculated from the $z_t = 0.75$ row in Table 1 is plotted as this value provides the best fit for the data.

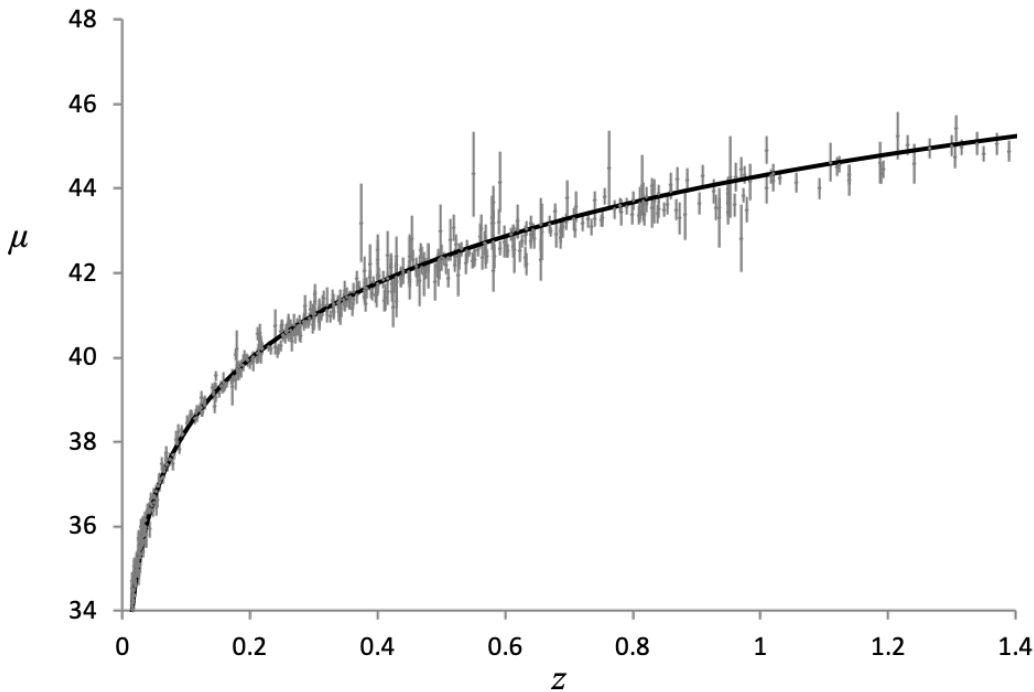


Figure 12. Distance Modulus vs. Redshift Plotted with Supernova Measurements

Figure 13 shows the same curve from Figure 12 for the Hubble diagram plotted out to higher redshifts with the quasar data from [5] also shown with error bars.

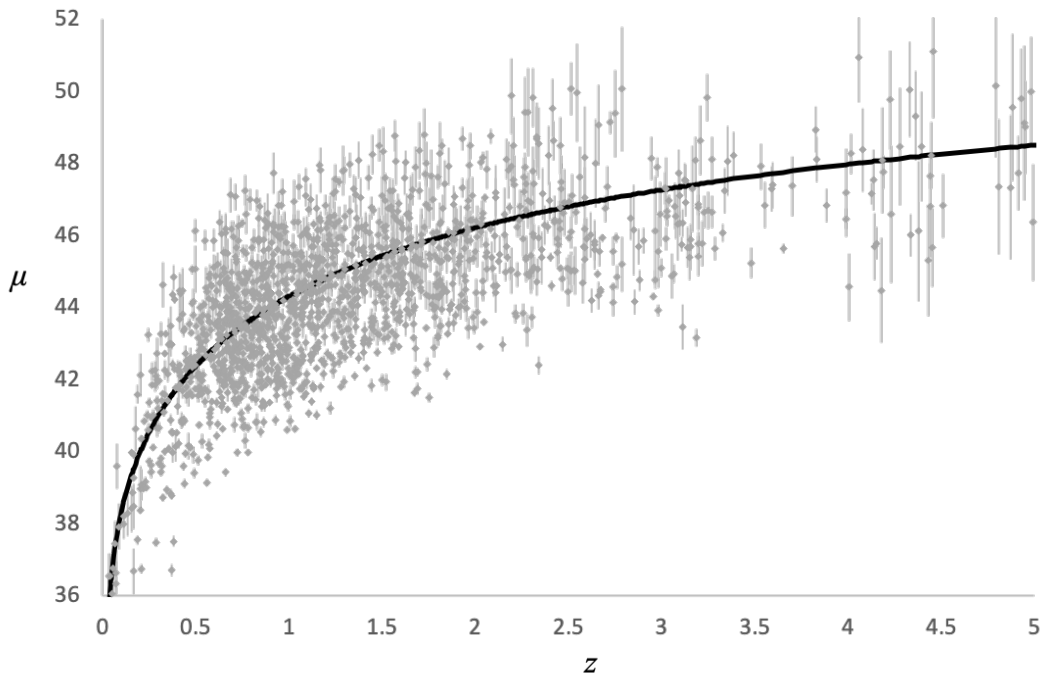


Figure 13. Distance Modulus vs. Redshift Plotted with Quasar Measurements

Figure 14 is a comparison of the Λ CDM model with the Schwarzschild model with the $z_t = 0.75$ transition redshift. As can be seen in this figure, both models are in very close agreement for the range of data available.

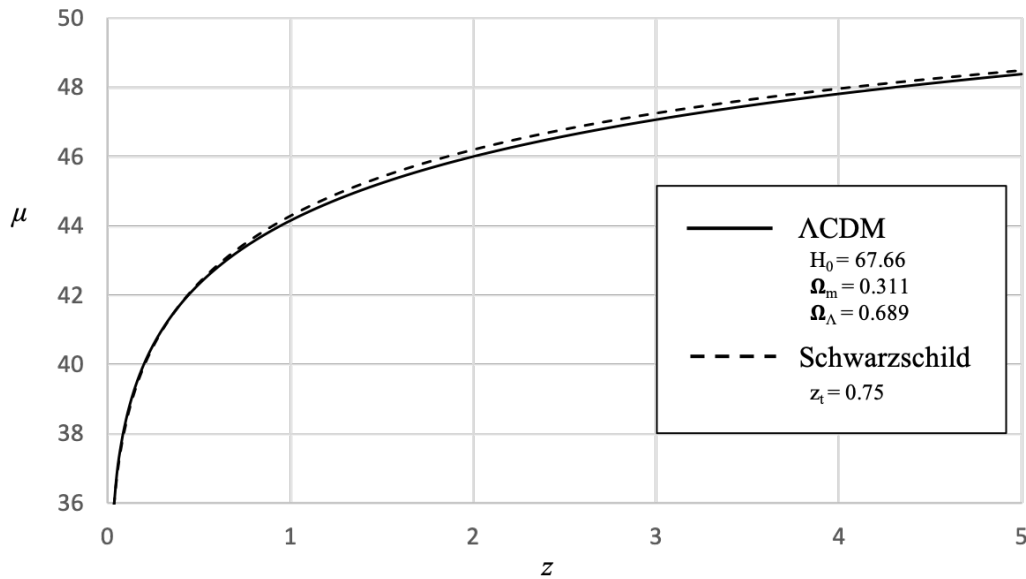


Figure 14. Distance Modulus vs. Redshift Comparison with Λ CDM

Finally, by subtracting r_0 from Equation 25 we can calculate the lookback time for a given redshift. Figure 15 shows the lookback time vs. redshift for the three transition redshifts from table 1.

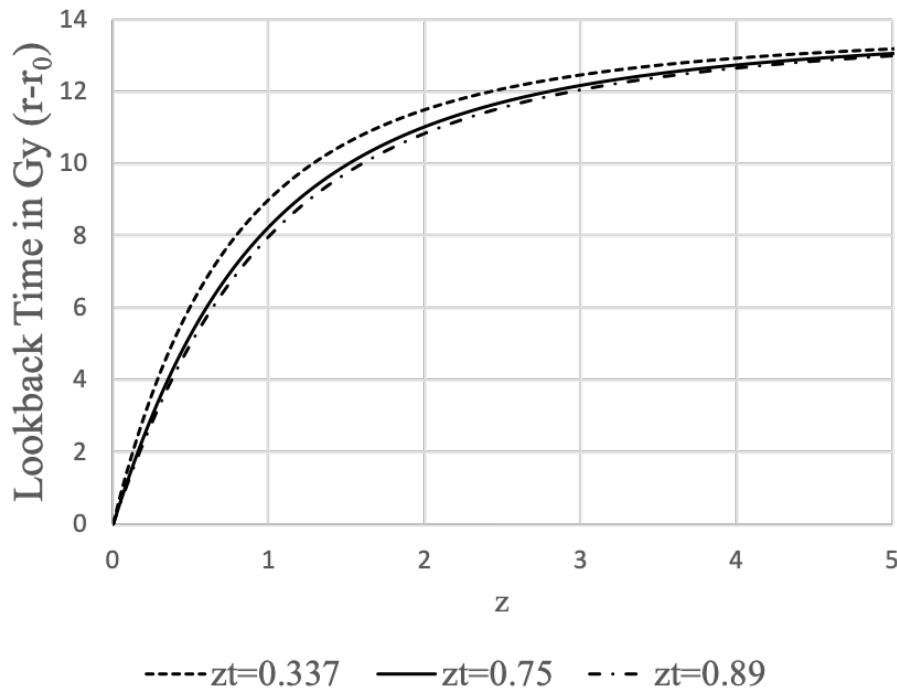


Figure 15. Lookback Time vs. Redshift

4.4. Behavior of Light in the Interior Metric

The path of light should also be affected by the angular term of the interior metric. When light is gravitationally lensed, its momentum vector changes direction, meaning it gains a non-zero $d\Omega$. We can see the precise behaviour of lensed light by looking at the geodesic equation for angular motion [1] (we will examine the case for planar rotation where $\theta = \frac{\pi}{2}$).

$$\frac{d^2\phi}{d\lambda^2} = -\frac{2}{r} \frac{d\phi}{d\lambda} \frac{dr}{d\lambda} \quad (35)$$

For light, we will use $\lambda = r$. If we consider light lensed by a galaxy, as the light passes the galaxy at some coordinate time r_0 , it will have some angular velocity $\dot{\phi}_0$ and initial angle ϕ_0 as it leaves the galaxy. It is currently assumed that the light then continues along a straight line as it leaves the gravitational field, but as we shall see, this is not the case. The ϕ_0 would be the angle caused only by the gravitational lensing, without any additional effects from the cosmological model (i.e. the angle we would expect when only taking into account the mass of the galaxy). Given these initial conditions, the solution to Equation 35 is:

$$\phi(r) = \phi_0 + \dot{\phi}_0 r_0 \left(1 - \frac{r_0}{r}\right) \quad (36)$$

Both the bracketed expression and $\dot{\phi}_0$ will always be negative (because dr is negative and $r_0 > r$) such that the second term is always positive. Therefore, the observed lensing angle will be increased by the amount $\dot{\phi}_0 r_0 \left(1 - \frac{r_0}{r}\right)$ as a result of this effect (where r is the coordinate time at which the light is observed). Furthermore, since $\frac{d\phi}{dr}$ for the light increases over time, the $\frac{dt}{dr}$ will correspondingly decrease as well and the result of this is that the increase in lensing angle over time will also result in a redshift of the light relative to unlensed light.

We see that the 'excess angle' is dependant on the lensing rate $\dot{\phi}_0$. So if we consider two cases where in one case, the light is gently lensed over a large distance/time by some angle ϕ_0 and in the other case, light is lensed by a more dense mass the same ϕ_0 , the lensing rate $\dot{\phi}_0$ would be higher in the second case relative to the first. So even though the pure gravitational lensing angle ϕ_0 would be the

same in both cases, the observed angle would be greater in the second case because the lensing rate ϕ_0 would be greater in that case.

5. The Antiverse at the Beginning of Time

We have to this point shown that the cosmological model of the Universe can be described as an FRW Universe which subsequently condenses into a Schwarzschild spacetime as described in the current work. But we must now consider the source of the initial FRW Universe.

Figure 16 shows the full Schwarzschild metric in Kruskal-Szekeres coordinates. The diagram can be split in two along the diagonal where in the top right half, forward time points up in both the interior and external regions while in the bottom left half, forward in time points down. The direction of positive space is also swapped when looking at the upper and lower halves. For the external metric, the radius increases to the right in the upper half and to the left in the lower half. For the interior metric, the spatial t coordinate goes from $-\infty$ to $+\infty$ from left to right in the upper half and from right to left in the lower half.

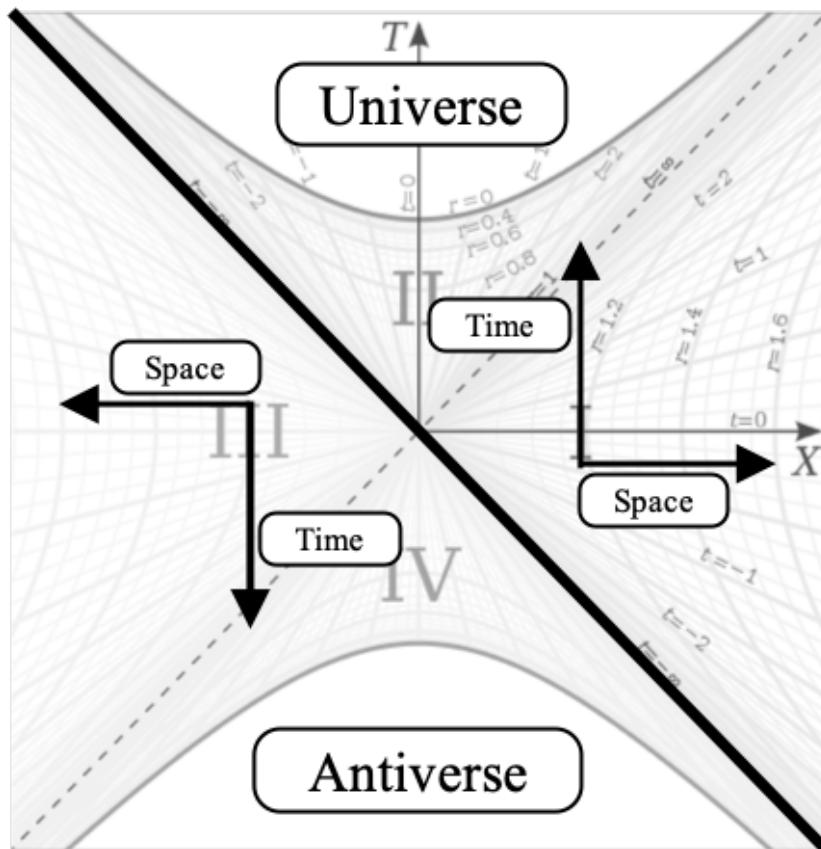


Figure 16. Universe and Antiverse

We can therefore conjecture that the diagram is describing both a Universe expanding up from the center and an Antiverse expanding down from the center, each one moving toward a singularity. We expect that the Antiverse is made of mostly anti-matter because the directions of both time and space are reversed relative to each other and therefore we expect the particles of the second Universe to have opposite charges relative to the first. This interpretation provides a resolution to the question of why we only tend to see matter in our Universe. It is because the equivalent amount of antimatter is contained in this mirror Universe. The lower hyperboloid sheet in Figure 2 therefore represents a 2D slice of the Antiverse at a given time. Thus, the pair of Universes satisfies CPT symmetry.

So we can think of the source of the Universe as being the intersection of the Universe and Antiverse. This intersection represents a pair production of Universe and Antiverse moving in positive

and negative time. The intersection is a point of infinite energy and temperature, like an engine generating the FRW Universe and Antiverse which each condense into their respective Schwarzschild Universe and Antiverse. This intersection would be represented by the $T = X = 0$ point in Figure 16.

In Figure 10, we showed the gravitational wells of Black Holes stretching back to this intersection point. We can imagine an identical picture mirrored in the horizontal axis representing the same situation in the Antiverse. Therefore, when a particle reaches an event horizon, it meets its antiparticle and annihilates with it. The light from this annihilation would then decompose back into matter and anti-matter particles that would begin falling again from $r = u$ into their respective Universe and Antiverse.

Putting all this together, we can think of the surface of the interior metric as a source of infinite energy at infinite temperature where the Universe and Antiverse intersect. Matter 'evaporates' from this surface, creating a fog we know as an FRW Universe. This fog subsequently cools and condenses into stars and galaxies analogous to clouds. In some regions, the matter in these clouds become so dense, the matter there falls back to the surface via the gravitational wells analogous to rain falling from the clouds. The matter then evaporates once again, starting the process over. So we can think of the Universe as a heat engine operating within an infinite temperature differential powered by the intersection of the Universe and Antiverse.

Appendix A Length Contraction in Kruskal-Szekeres Coordinates

The Kruskal-Szekeres coordinates are the maximally extended coordinates for the Schwarzschild metric. The coordinate definitions and metric in Kruskal-Szekeres coordinates are given below (derivation of the coordinate definitions and metric can be found in reference [1] where $v = T$ and $u = X$).

$$\begin{aligned} T &= \sqrt{\left(\frac{r}{r_s} - 1\right)e^{\frac{r}{r_s}}} \sinh\left(\frac{t}{2r_s}\right) \\ X &= \sqrt{\left(\frac{r}{r_s} - 1\right)e^{\frac{r}{r_s}}} \cosh\left(\frac{t}{2r_s}\right) \end{aligned} \quad (\text{A1})$$

With the full metric in Kruskal-Szekeres coordinates given by:

$$d\tau^2 = \frac{4r_s^3}{r} e^{-\frac{r}{r_s}} (dT^2 - dX^2) - r^2 d\Omega^2 \quad (\text{A2})$$

The coordinate chart for this metric is given in Figure 3. Light-like geodesics are 45 degree lines on this diagram. Let us take the differentials of T and X in equations A1:

$$\begin{aligned} dX &= \frac{\partial X}{\partial r} dr + \frac{\partial X}{\partial t} dt \\ dT &= \frac{\partial T}{\partial r} dr + \frac{\partial T}{\partial t} dt \end{aligned} \quad (\text{A3})$$

Calculating the partial derivatives, rearranging and defining $R \equiv \frac{re^{\frac{r}{r_s}}}{2r_s^2 \sqrt{(\frac{r}{r_s} - 1)e^{\frac{r}{r_s}}}}$ we get:

$$\begin{aligned} \frac{dX}{dt} &= R \left[\frac{dr}{dt} \cosh\left(\frac{t}{2r_s}\right) + \left(1 - \frac{r_s}{r}\right) \sinh\left(\frac{t}{2r_s}\right) \right] \\ \frac{dT}{dt} &= R \left[\frac{dr}{dt} \sinh\left(\frac{t}{2r_s}\right) + \left(1 - \frac{r_s}{r}\right) \cosh\left(\frac{t}{2r_s}\right) \right] \end{aligned} \quad (\text{A4})$$

Next, we need to calculate $\frac{dX}{dT}$ from equations A4 by factoring out $(1 - \frac{r_s}{r}) \cosh\left(\frac{t}{2r_s}\right)$ from each equation and dividing:

$$\frac{dX}{dT} = \frac{dX}{dt} \frac{dt}{dT} = \frac{\frac{dr}{dt} (1 - \frac{r_s}{r})^{-1} + \tanh\left(\frac{t}{2r_s}\right)}{\frac{dr}{dt} (1 - \frac{r_s}{r})^{-1} \tanh\left(\frac{t}{2r_s}\right) + 1} \quad (\text{A5})$$

Next, we make the following definition:

$$\left(\frac{dX}{dT}\right)_0 \equiv \tanh\left(\frac{t}{2r_s}\right) \quad (\text{A6})$$

This is the derivative of the rest frame at t since plugging $\frac{dr}{dt} = 0$ into equation A5, we get $\frac{dX}{dT} = \tanh\left(\frac{t}{2r_s}\right)$.

Now consider the hyperbolas of constant r in region I of Figure 3 which represent the worldlines of rest observers in Kruskal-Szekeres coordinates. In these coordinates, rest observers accelerate over time as evidenced by the fact that their worldlines are hyperbolas in these coordinates. If we consider the X position of a rest observer at some $t > 0$, we see that its X -coordinate is given by $X = X_0 \cosh\left(\frac{t}{2r_s}\right)$ where X_0 is the X coordinate of the rest observer at r when $t = 0$ ($X_0 = \sqrt{\left(\frac{r}{r_s} - 1\right) e^{\frac{r}{r_s}}}$). At $t > 0$, the rest observer is moving with some velocity relative to itself at $t = 0$ on this coordinate chart. Therefore, we should expect that the X coordinate will be length contracted as t increases in the rest frame in Kruskal-Szekeres coordinates. The length contracted value of X in the rest frame at r and $t > 0$ is given by:

$$\begin{aligned} X' &= X \sqrt{1 - \left(\frac{dX}{dT}\right)_0^2} \\ &= X_0 \cosh\left(\frac{t}{2r_s}\right) \sqrt{1 - \tanh^2\left(\frac{t}{2r_s}\right)} \\ &= X_0 \cosh\left(\frac{t}{2r_s}\right) \frac{1}{\cosh\left(\frac{t}{2r_s}\right)} \\ &= X_0 \end{aligned} \quad (\text{A7})$$

Where $\left(\frac{dX}{dT}\right)_0$ is the effective velocity of the rest observer in Kruskal-Szekeres coordinates as defined in equation A6.

So even though the X coordinate grows for an observer at rest in the Kruskal-Szekeres coordinate chart, when we shift to the frame of the rest observer by taking into account the length contraction of the Kruskal-Szekeres coordinates in that frame, we see that we end up back at $t = 0$. This means that the surface of the event horizon of a Black Hole can always be shifted to $X = T = 0$ on the Kruskal-Szekeres coordinate chart by taking length contraction into account. This amounts to hyperbolically rotating the spacetime such that the 'present' is always at $t = 0$ on the coordinate chart.

Appendix B CMB Temperature and Absolute Simultaneity

The Minkowski spacetime of Special Relativity has no intrinsic geometric features that can be used for reference. Since it is everywhere and at all times uniform, one cannot define a universal 'present' in Special Relativity, leading to the relativity of simultaneity. To put it more precisely, it is not possible for causally disconnected observers in Special Relativity to synchronize their clocks.

But the Schwarzschild geometry does have intrinsic geometrical features. Importantly, the intrinsically spherical nature of time in the interior metric provides causally disconnected observers the ability to synchronize their clocks by agreeing ahead of time to start their clocks when they are

at a specific r (in the interior metric). This allows us to order events absolutely regardless of their spacetime separation because each event occurs at a specific r and the r of different events can be used to objectively order the events in time.

In our Universe, this amounts to agreeing to start the clocks when the CMB monopole is at a specific temperature. This works because the CMB temperature is related to the scale factor a of the Universe, which itself is a function of r .

Since r is not itself directly measurable, it is more useful in a practical sense to use the temperature of the Universe as a measure of cosmological time. The CMB is a perfect black body and its temperature is inversely proportional to the scale factor a . We can relate them precisely with:

$$\frac{T}{T_0} = \frac{a_0}{a} \quad (\text{A8})$$

Where T and a are the CMB monopole temperature and scale factor at any time r and T_0 and a_0 are the temperature and scale factor at some reference time r_0 . To keep the equations simple, we can choose the reference scale factor to be 1 and use a temperature scale such that the CMB monopole temperature at that time is also 1. In section 4, it was shown that the current scale factor is very close to 1 and the current CMB monopole temperature is 2.725K. Therefore, if we measure temperature in units of Kelvin divided by 2.725, we get a unitless temperature scale and the relationship between T and r becomes

$$T = \frac{1}{a} = \frac{1}{\sqrt{\frac{u}{r} - 1}} \quad (\text{A9})$$

and

$$r = \frac{u}{T^2 + 1} \quad (\text{A10})$$

Furthermore, we have an estimate for u from section 4 of 27.3Gy. If we work in units of time where $u = 1$ (such that one of these units of time equals 27.3Gy), then we can also drop the u from the equations (so we are working with a unitless timescale).

Taking the derivative of equation A10, we obtain:

$$dr = \frac{2T}{(T^2 + 1)^2} dT \quad (\text{A11})$$

Substituting equations A9 and A11 into equation 1 we get the metric as a function of CMB monopole temperature T :

$$d\tau^2 = \frac{4T^4}{(T^2 + 1)^4} dT^2 - \frac{1}{T^2} dt^2 - \frac{T^4}{(T^2 + 1)^2} d\Omega^2 \quad (\text{A12})$$

In these coordinates, $r \rightarrow 0$ as $T \rightarrow 0$ and $r \rightarrow u$ as $T \rightarrow \infty$. So by using the CMB monopole temperature as a measure of cosmological time, we get a clearer understanding of time dilation. We can establish a universal rest frame in the Schwarzschild metric (the co-moving observer for whom the CMB has only a monopole), against which we can measure all motion. The velocity of a frame relative to the co-moving frame can be determined by the CMB dipole observable in that frame. Therefore, the CMB dipole seen in a given frame tells that frame its absolute velocity. This absolute velocity is not only increased motion through space relative to the co-moving observer, but also increased motion through time. A reference frame with a non-zero velocity will see the CMB monopole cool more quickly according to their clock relative to the co-moving observer as a result of the time dilation. So we can describe time dilation between two frames in our Universe as the difference in the rate at which the CMB monopole cools (or heats up in the collapsing Universe) according to the clock in each frame. A moving frame is not only moving faster through space than the co-moving observer, but also faster through cosmological time measured using the CMB monopole temperature.

Therefore, time dilation is better thought of as one frame moving faster through cosmological time than another, rather than one frame's clock 'ticking more slowly' than the other. And, in the author's opinion, using the CMB monopole temperature as the measure of cosmological time allows for a more intuitive description of the time dilation.

References

1. S. M. Carroll, Lecture notes on general relativity (1997), arXiv:9712019v1 [gr-qc].
2. J. A. S. Lima, J. F. Jesus, R. C. Santos, and M. S. S. Gill, Is the transition redshift a new cosmological number? (2014), arXiv:1205.4688 [astro-ph.CO].
3. H. E. Bond, E. P. Nelan, D. A. VandenBerg, G. H. Schaefer, and D. Harmer, The Astrophysical Journal 765, L12 (2013).
4. S. C. Project, Supernova cosmology project - union2.1 compilation magnitude vs. redshift table (for your own cosmology fitter), <http://supernova.lbl.gov/Union/figures/SCPUnion2.1muvsz.txt> (2010), accessed on Aug. 17, 2017.
5. G. Risaliti and E. Lusso, Cosmological constraints from the hubble diagram of quasars at high redshifts (2018), arXiv:1811.02590 [astro-ph.CO].
6. Figures 1 and 13 are modifications of: 'kruskal diagram of schwarzschild chart' by dr greg. licensed under cc by-sa 3.0 via wikipedia commons, http://commons.wikimedia.org/wiki/File:Kruskal_diagram_of_Schwarzschild_chart.svg /File:Kruskal diagram of Schwarzschild chart.svg (Accessed in 2017).

Disclaimer/Publisher's Note: The statements, opinions and data contained in all publications are solely those of the individual author(s) and contributor(s) and not of MDPI and/or the editor(s). MDPI and/or the editor(s) disclaim responsibility for any injury to people or property resulting from any ideas, methods, instructions or products referred to in the content.